

# Enabling Reconfiguration-Communication Overlap for Collective Communication in Optical Networks

CHANGBO WU, University of Science and Technology of China, China and Shanghai Innovation Institute, China

ZHUOLONG YU, University of Science and Technology of China, China

GONGMING ZHAO, University of Science and Technology of China, China

HONGLI XU, University of Science and Technology of China, China

Collective communication (CC) is critical for scaling distributed machine learning (DML). The predictable traffic patterns of DML present a great opportunity for applying optical network technologies. Optical networks with reconfigurable topologies promise high bandwidth and low latency for collective communications. However, existing approaches face inherent limitations: static topologies are inefficient for dynamic communication patterns within CC algorithm, while frequent topology reconfiguration matching every step of the algorithm incurs significant overhead.

In this paper, we propose SWOT, a demand-aware optical network framework that employs “intra-collective reconfiguration” to dynamically align network resources with CC traffic patterns. SWOT hides reconfiguration latency by overlapping it with data transmission through three key techniques: *Heterogeneous Message Splitting*, *Asynchronous Overlapping*, and *Topology Bypassing*. Extensive simulations demonstrate that SWOT reduces communication completion time up to 89.7% across diverse CC algorithm compared to static baselines, demonstrating strong robustness to varying optical resources and reconfiguration delay.

## 1 Introduction

The scaling laws[15] dictate that the AI model size and training data size are critical factors determining the model capability. To achieve high model performance and capability, distributed machine learning (DML) has emerged as an essential strategy. Efficient DML relies on distributed computing clusters with high bandwidth, low end-to-end latency, and high scalability[13, 27].

In recent decades, significant investments have driven the development of optical network technologies, with optical circuit switches (OCSs) now being widely deployed in modern data centers[6, 14, 17, 19, 34]. In DML training, the communication pattern is dominated by predictable, high-throughput collective communication (CC) operations, which makes it particularly well suited for leveraging the reconfigurability and high-capacity switching of optical networks[11, 14, 16, 28]. However, existing approaches are constrained either spatially, by the limited optical degree of static topologies, or temporally, by the non-negligible latency of optical reconfiguration.

Current optical interconnect-based CC schemes (e.g., TopoOpt [28]) predominantly adopt a “one-shot” reconfiguration strategy. By establishing a fixed topology that persists throughout the collective operation, these approaches effectively avoid the overhead introduced by reconfiguring the optical network. However, this static paradigm faces a fundamental scalability barrier: modern DML workloads increasingly rely on more efficient but complex CC implementation (e.g., Pairwise All-to-All Algorithm, Rabenseifner’s algorithm for AllReduce) with highly dynamic, time-varying connectivity demands. Embedding the union of these diverse demands into a single static optical topology often exceeds the physical optical degree of the network. Consequently, systems are compelled to rely on suboptimal static-friendly algorithms or indirect multi-hop routing, causing non-negligible performance degradation and compromising training efficiency.

---

Authors’ Contact Information: Changbo Wu, wuchangbo@mail.ustc.edu.cn, University of Science and Technology of China, Hefei, Anhui, China and Shanghai Innovation Institute, Shanghai, China; Zhuolong Yu, zhuolongyu@ustc.edu.cn, University of Science and Technology of China, Hefei, Anhui, China; Gongming Zhao, gmzhao@ustc.edu.cn, University of Science and Technology of China, Hefei, Anhui, China; Hongli Xu, xuhongli@ustc.edu.cn, University of Science and Technology of China, Hefei, Anhui, China.

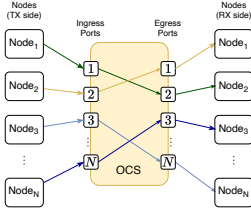


Fig. 1. Example of OCS interconnect. Left and right sides denote the same nodes (TX and RX paths, respectively).

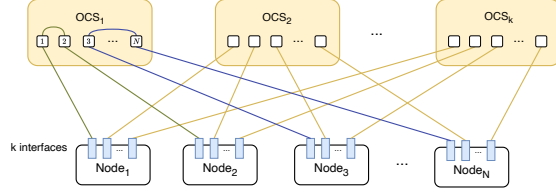


Fig. 2. Example of optical network topology, where  $OCS_1$  is reconfigured matching Fig. 1.

To effectively support these dynamic communication patterns, an alternative direction is to enable “intra-collective reconfiguration” — dynamically adapt network topology to match the specific demand of each algorithmic step. However, the naive implementation of this approach (which we refer to as *Strawman*) faces a harsh reality: optical switching is not instant. Standard OCS devices incur a non-negligible latency  $T_{\text{reconf}}$  to complete topology reconfiguration once. If the network strictly synchronizes reconfiguration with every communication step, the system enters a “stop-and-wait” cycle. For multi-step algorithms, the accumulated reconfiguration overhead often outweighs the advanced CC algorithm benefits, rendering this approach impractical.

We argue that the key to unlocking the potential of optical networks lies in enabling “intra-collective reconfiguration” without paying the full reconfiguration latency cost. To address these challenges, we propose SWOT, a demand-aware optical network framework that makes “intra-collective reconfiguration” practical. SWOT incorporates three key mechanisms: (1) **Heterogeneous Message Splitting**: It strategically adjusts message splits to create temporal windows for overlap and bypassing; (2) **Asynchronous Overlapping**: It removes strict synchronization across parallel optical planes, enabling some planes/OCSs to reconfigure while others continue transmitting; (3) **Topology Bypassing**: It selectively bypasses intermediate reconfiguration stages for certain planes, directly eliminating switching overheads.

Our contributions are summarized as follows:

- We identify fundamental limitations in the current optical CC design space, where static strategies are constrained by limited optical degrees and naive dynamic strategies incur prohibitive reconfiguration latency.
- We propose SWOT, a scheduling framework that leverages message splitting, overlap, and bypassing techniques to mask reconfiguration latency.
- We perform a comprehensive evaluation covering efficiency and scalability across CC primitives, and hardware sensitivity. Results show SWOT reduces communication time up to 89.7% across diverse primitives and exhibits robustness against varying optical degrees ( $k$ ) and reconfiguration latencies ( $T_{\text{reconf}}$ ).

## 2 Background & Motivation

### 2.1 Background

**2.1.1 Optical Network and Optical Circuit Switch.** Modern optical networks deliver *tera-scale bandwidth* and *deterministic  $\mu\text{s}$ -level latency* through direct photonic signal propagation, bypassing electronic packet processing bottlenecks. Among various optical switching technologies, Optical Circuit Switching (OCS) achieves this by creating an optical path, or “circuit”, between the source and destination. As shown in Fig 1, an  $N \times N$  OCS establishes a one-to-one mapping between its ingress and egress ports. This functionality can be realized using different physical technologies, such as MEMS mirrors, liquid crystal or thermo-optic switches. In a MEMS-based OCS, a representative

example, the connectivity is physically realized by an  $N \times N$  mirror array that physically steers optical beams to link the designated ingress and egress ports. Notably, this intrinsic **bijective mapping** is a fundamental property of OCS regardless of the underlying hardware, and can be uniformly formalized as a permutation matrix  $\mathbf{P} \in \{0, 1\}^{N \times N}$  where  $p_{ij} = 1$  iff input  $i$  connects to output  $j$ .

A defining feature of OCS is its **reconfigurability** – the ability to dynamically change the permutation  $\mathbf{P}$  to match evolving traffic patterns. However, this flexibility comes with a switching overhead, denoted as **reconfiguration latency** ( $T_{\text{recfg}}$ ). This latency is determined by the underlying physical technology. Recent hardware advances have expanded the achievable range of OCS reconfiguration latency to cover scales from 10 ns [6] to 10  $\mu\text{s}$  [20] to 10 ms. However, optical technologies face a fundamental tradeoff among three key parameters: port-count, reconfiguration latency, and insertion loss [11]. Specifically, OCS devices achieving ns-to- $\mu\text{s}$ -scale reconfiguration times typically suffer from either severely limited port counts or high insertion loss, making  $\mu\text{s}$ -to-ms-scale OCS devices more practical for large-scale GPU cluster interconnects. This makes the overhead of reconfiguration non-negligible during collective operations in optical-interconnected clusters.

Fig. 2 illustrates the physical view of the direct-connect optical topology adopted in this work. The cluster consists of  $N$  computing nodes interconnected through  $k$  parallel OCS devices. Each node possesses  $k$  optical interfaces, where the  $j$ -th interface of every node is physically connected to a distinct port on the  $j$ -th OCS ( $OCS_j$ ). This structure effectively creates  $k$  parallel optical planes, where  $OCS_j$  is responsible for establishing connections between the  $j$ -th interfaces of any pair of nodes. By configuring the internal port mappings of these  $k$  OCSs, specific logical topologies (e.g., rings, tori, or random graphs) can be constructed over the physical infrastructure.

The optical degree  $k$  is a critical parameter defining the network’s parallelism. It can be scaled by equipping nodes with additional physical network adapters or, more commonly, by leveraging the *Port Splitting* (or *Breakout*) capabilities inherent in modern high-performance NICs. Port splitting allows a single high-bandwidth physical port to be logically reconfigured into multiple independent, lower-bandwidth interfaces to meet diverse networking demands. For instance, the NVIDIA C8180 ConnectX-8 SuperNIC [4], featuring a single-port OSFP module capable of 800 Gb/s, can be reconfigured from its default configuration to support two 400 GbE ports ( $k=2$ ) or up to eight 100 GbE ports ( $k=8$ ). Similar capabilities are widely supported by other adapters, such as the Intel Ethernet 800 Series [3], Broadcom NetXtreme [1], and Marvell FastLinQ 45000 [2].

**2.1.2 Collective Communication.** Modern DML workloads increasingly adopt hybrid parallelism strategies to handle the heavy computational load, combining data parallelism, tensor parallelism, expert parallelism, context parallelism etc[32]. These parallelization schemes rely on collective communication (CC) primitives (e.g., AllReduce, AllGather, All-to-All) as the coordination backbone for synchronizing gradients, parameters, and intermediate tensors across distributed accelerators.

It is crucial to distinguish between **CC primitives** and **CC algorithms**. CC primitives (e.g., AllReduce, AllGather, All-to-All) define the high-level communication semantics—specifying what data needs to be aggregated or exchanged. Each primitive can be implemented by multiple *CC algorithms* (e.g., Ring, Tree, Recursive-Doubling, Bruck), each optimized for different message sizes, node counts ( $p$ ), and network topologies.

The performance of these algorithms is typically modeled using the  $\alpha - \beta$  cost model [12], where  $\alpha$  represents the fixed per-message latency (including software overhead and propagation delay) and  $\beta$  represents the per-byte transmission time (inverse of bandwidth). Despite its simplicity, this model remains widely accepted in recent state-of-the-art literature [8, 9, 23–26, 31, 33] and has

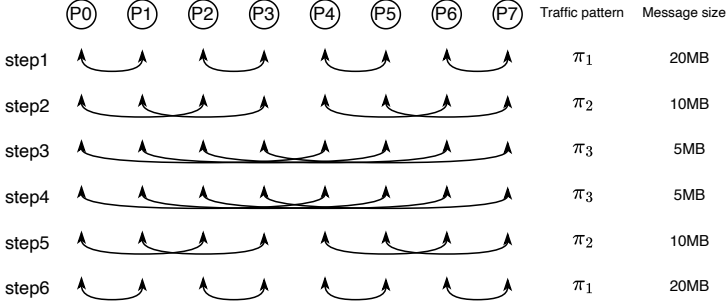


Fig. 3. For an 8-node AllReduce with a 40 MB payload, Rabenseifner’s algorithm proceeds in six communication steps. Each node splits the data into eight 5 MB segments. Steps 1–3 implement a reduce-scatter using recursive halving with three bijective pairings, after which node  $P_i$  owns the reduced  $i$ -th segment. Steps 4–6 perform an allgather using recursive doubling to disseminate these segments to all nodes. The *Message size* column on the right shows the amount of data exchanged at each stage of every step.

been empirically verified via linear regression on physical testbeds [33], confirming its fidelity for modeling modern high-speed interconnects.

Different algorithms dominate different regimes based on their  $\alpha$  and  $\beta$  complexities. For example, Ring-based algorithms are bandwidth-optimal (minimized  $\beta$  term) but suffer from high latency scaling linearly with  $p$ , making them suitable for large messages. Conversely, algorithms like Bruck or Recursive-Doubling optimize latency ( $O(\log p)$  steps) but may induce bandwidth contention, making them ideal for small messages. Production libraries (e.g., NCCL, MPI) dynamically select the *Best-Known Algorithm* based on runtime conditions to minimize the estimated completion time.

A key characteristic of CC lies in its **multi-step execution**: each collective algorithm decomposes into sequential communication steps where every node participates in exclusively pairwise data transfers at each step. This avoids simultaneous many-to-one or one-to-many traffic patterns that create congestion hotspots. The multi-step communication patterns can be formalized as sequences of **bijective pairings**. For  $N = 8$  nodes labeled  $\{0, \dots, 7\}$ , let  $\pi_t : [N] \rightarrow [N]$  denote the pairing function at step  $t$ , where each node  $i$  communicates with a peer  $\pi_t(i)$ . Crucially, these steps are strictly sequential: step  $t + 1$  relies on the data reduced or collected in step  $t$ , creating a global synchronization barrier between steps.

**AllReduce (Ring)**: At each step, node  $i$  sends its data to  $\pi_t(i) = (i + 1) \bmod 8$ , propagating partial reductions through adjacent nodes in a circular pipeline.

**AllReduce (Rabenseifner’s Algorithm[22])**: Fig. 3 shows the pattern of  $\log_2 N$ -step ( $N = 8$ ) Reduce-Scatter phase.

- Step 1:  $\pi_1(i) = i \oplus 1$  (2-node microgroups:  $\{0 \leftrightarrow 1, 2 \leftrightarrow 3, 4 \leftrightarrow 5, 6 \leftrightarrow 7\}$ )
- Step 2:  $\pi_2(i) = i \oplus 2$  (4-node subgroups:  $\{0 \leftrightarrow 2, 1 \leftrightarrow 3, 4 \leftrightarrow 6, 5 \leftrightarrow 7\}$ )
- Step 3:  $\pi_3(i) = i \oplus 4$  (Cross-group:  $\{0 \leftrightarrow 4, 1 \leftrightarrow 5, 2 \leftrightarrow 6, 3 \leftrightarrow 7\}$ )

The Allgather phase reverses this pattern in next  $\log_2 N$  steps.

**All-to-All (Pairwise Exchange)**: This algorithm employs  $N - 1$  steps to progressively disseminate data blocks: At each step  $t \in [1, 2, \dots, N - 1]$ , node  $i$  sends the data block to  $\pi_t(i) = (i + t) \bmod 8$ , accumulating one new block per step.

**2.1.3 Mapping Collective Algorithms to Optical Substrates.** The multi-step nature of CC algorithms (described in §2.1.2) introduces a **time-varying connectivity demand**. Formally, a collective algorithm can be viewed as a sequence of bijective pairings  $\Pi = \{\pi_1, \pi_2, \dots, \pi_{|\Pi|}\}$ , where  $\pi_t$  represents the specific logical topology required at algorithmic step  $t$ . To support this demand, the optical network provides a sequence of physical OCS configurations  $C = \{\mathbf{P}_1, \mathbf{P}_2, \dots, \mathbf{P}_{|C|}\}$ , where

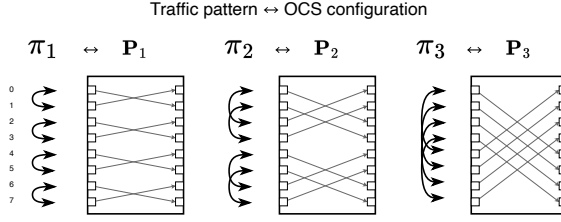


Fig. 4. OCS configuration corresponding to traffic pattern in 8-node Rabenseifner’s AllReduce (see Fig 3)

each  $P_j$  represents a set of established circuit permutations. For instance, as illustrated in Fig. 4, each bijective pairing stage ( $\pi_1, \pi_2, \pi_3$ ) requires a corresponding OCS bijective mapping ( $P_1, P_2, P_3$ ).

The fundamental challenge lies in embedding the logical sequence  $\Pi$  into the physical sequence  $C$  under the constraints of the optical hardware. A valid mapping ensures that for any algorithmic step  $t$ , the required connectivity  $\pi_t$  is supported by the active physical configuration. This mapping can be achieved through two distinct dimensions:

- **Spatial Reservation:** Provisioning a physical topology that simultaneously contains links for multiple (or all) logical steps. This relies on the spatial parallelism (optical degree  $k$ ) to accommodate the union of demands.
- **Temporal Reconfiguration:** Dynamically switching the physical topology over time to match the changing logical demands step-by-step. This relies on the temporal agility ( $T_{\text{reconf}}$ ) of the OCS.

## 2.2 Current Solutions and Limitations

Based on the mapping dimensions discussed in §2.1.3, the current design space for optical collective communication is polarized, with practical solutions clustering at the static end.

**1. The Status Quo: Static Pre-configuration (“One-shot”):** Approaches like TopoOpt [28] prioritize spatial reservation, provisioning a single, static topology for the entire collective operation, and even the whole training iteration (*i.e.*,  $|C| = k$ , where  $k$  is the optical degree, typically  $k \in \{2, 4, 8\}$ ). To ensure connectivity throughout the collective operation without reconfiguration, this static configurations  $\bigcup_{i=1}^k P_i$  must structurally embed the *union* of all logical pairings ( $\bigcup_{t=1}^{|\Pi|} \pi_t$ ). While effective for sparse patterns like Ring-AllReduce, this approach fails for complex algorithms. For instance, the Pairwise-Exchange All-to-All algorithm implies a union graph equivalent to a fully connected clique ( $K_N$ ). Supporting such a dense graph on nodes with limited constant-level  $k$  ( $k \ll N$ ) is physically impossible. Consequently, “One-shot” schemes are compelled to either discard communication-efficient algorithms that exhibit dynamic patterns in favor of suboptimal static-friendly variants, or rely on indirect multi-hop routing to satisfy connectivity. Both approaches inevitably lead to significant performance degradation compared to direct transmission.

**2. The Hypothetical Alternative: Naive Intra-Collective Reconfiguration.** To overcome the limitations of static topologies, one might consider exploiting the temporal dimension by strictly switching the configuration to match each algorithmic step (*i.e.*,  $|C| = |\Pi|$ ). We refer to this hypothetical baseline as the naive intra-collective reconfiguration (Strawman-ICR). While this maximizes spatial efficiency by dedicating all optical links to the current demand, it suffers from prohibitive temporal overhead. Since standard OCS devices incur a reconfiguration latency  $T_{\text{reconf}}$  (*e.g.*,  $200\mu\text{s}$ ), pausing communication at every step introduces a cumulative “stop-and-wait” penalty of  $|\Pi| \times T_{\text{reconf}}$ . As shown in our later analysis (§3.1), this latency penalty often outweighs the bandwidth benefits, rendering the strategy impractical for sequences with many steps.

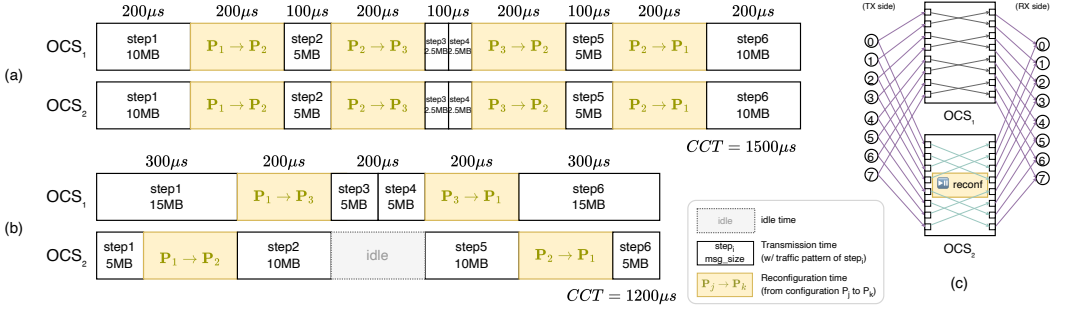


Fig. 5. Design Intuition of reconfiguration-communication overlapping design. Communication-reconfiguration timeline for 8-node AllReduce in optical network: (a) naive intra-collective reconfiguration incurs cumulative 800  $\mu s$  switching overhead, (b) SWOT’s overlap-optimized approach reduces CCT by 20% through partial circuit updates during transmissions (Illustrated in (c)). Configuration details (400Gbps links, 200  $\mu s$  reconfiguration delay), traffic patterns and required OCS configurations shown in Fig. 3 and Fig. 4.

**Goal of SWOT:** Existing solutions are fundamentally constrained by the physical properties of optical circuit switches (OCSs): static topologies are limited by optical degree (spatial constraint), while naive dynamic approaches are bottlenecked by reconfiguration latency (temporal constraint). SWOT aims to bridge this gap by exploring the design space in between—dynamically scheduling partial reconfigurations and overlapping them with data transmission—thereby making intra-collective reconfiguration practical.

### 3 SWOT Design

#### 3.1 Design Intuition

To overcome the limitations highlighted in §2.2, SWOT employs a demand-aware scheduling paradigm. We revisit the 8-node Rabenseifner’s AllReduce example from §2.1.2, with SWOT and the naive intra-collective reconfiguration approaches. Fig. 5 depicts the corresponding timelines under  $k = 2$  OCS planes. Analysis of the traffic patterns in Fig. 4 reveals that the collective operation requires a specific sequence of topological configurations:  $P_1 \rightarrow P_2 \rightarrow P_3 \rightarrow P_3 \rightarrow P_2 \rightarrow P_1$ , which directly correspond to the Reduce-Scatter and AllGather phases.

**The Inefficiency of Lockstep Scheduling (Fig. 5(a)).** Fig. 5(a) depicts the timeline of the naive intra-collective reconfiguration (Strawman-ICR). In this paradigm, the two OCS planes operate in *lockstep*: they serve the same communication step simultaneously and reconfigure synchronously. For instance, at Step 1, the 20MB traffic is evenly split between  $OCS_1$  and  $OCS_2$  (10MB each), taking 200  $\mu s$  to transmit. Crucially, before Step 2 can begin, *both* OCSs must stop and reconfigure from  $P_1$  to  $P_2$ , incurring a global penalty of  $T_{\text{refcg}} = 200 \mu s$ . This “stop-and-wait” cycle repeats for every topological transition. Consequently, the total Communication Completion Time (CCT) is dominated by the accumulated reconfiguration overhead:  $CCT = \sum t_{\text{trans}} + 4 \times T_{\text{refcg}} = 700 \mu s + 800 \mu s = 1500 \mu s$ . Here, reconfiguration accounts for 53.3% of the total time, severely limiting system efficiency. (Note: In this example, we omit the end-to-end base latency  $T_{\text{lat}}$  for simplicity, as it is negligible compared to both reconfiguration overhead  $T_{\text{refcg}}$  and transmission time.)

**Optimization via Asynchrony and Bypassing (Fig. 5(b)).** The root cause of the inefficiency above is the rigid synchronization. SWOT breaks this rigid synchronization, achieving performance gains through three synergetic mechanisms:

- (1) **Heterogeneous Message Splitting:** SWOT dedicatedly split the message and distributes the workload unevenly to each OCS. For example, in step 1, it assigns a larger chunk (15MB) to  $OCS_1$  and a smaller chunk (5MB) to  $OCS_2$ .

Table 1. Summary of Key Notations

Symbol	Type	Description
<i>Decision Variables</i>		
$d_{i,j}$	$\mathbb{R}^+$	Msg/Data volume assigned to OCS $j$ at step $i$
$r_{i,j}$	$\{0, 1\}$	1 if OCS $j$ needs reconfiguration at step $i$
$t_{\text{start}_{i,j}}$	$\mathbb{R}^+$	Transmission start time on OCS $j$ at step $i$
$t_{\text{end}_{i,j}}$	$\mathbb{R}^+$	Transmission end time on OCS $j$ at step $i$
$t_{\text{reconf}_{s_{i,j}}}$	$\mathbb{R}^+$	Reconfig start time for OCS $j$ at step $i$
$t_{\text{reconf}_{e_{i,j}}}$	$\mathbb{R}^+$	Reconfig end time for OCS $j$ at step $i$
<i>Intermediate Variables</i>		
$u_{i,j}$	$\{0, 1\}$	1 if OCS $j$ is used at step $i$ , 0 otherwise
$s_{i,j}$	$\{0, 1\}$	1 if OCS $j$ 's current config matches step $i$
$t_{\text{prev}_{e_{i,j}}}$	$\mathbb{R}^+$	last completion time of previous activities (trans / reconf) in OCS $j$ before step $i$
$t_{\text{step}_{e_i}}$	$\mathbb{R}^+$	Completion time of communication step $i$
$\text{last\_cfg}_{i,j}$	$\mathbb{N}$	Previous configuration of OCS $j$ at step $i$
<i>Parameters</i>		
$m_i$	$\mathbb{R}^+$	Total data volume required at step $i$
$B$	$\mathbb{R}^+$	OCS port bandwidth (Gbps)
$T_{\text{lat}}$	$\mathbb{R}^+$	End-to-end base latency (propagation + processing)
$T_{\text{reconf}}$	$\mathbb{R}^+$	OCS reconfiguration latency
$M$	$\mathbb{R}^+$	Large constant value for big-M method [10]
$\text{cfg}_i$	$\mathbb{N}$	Current configuration pattern at step $i$

- (2) **Asynchronous Overlapping:** The uneven split creates a time window.  $OCS_2$  finishes its small chunk early (at  $t = 100\mu\text{s}$ ) and immediately begins reconfiguring. By the time  $OCS_1$  finishes Step 1 (at  $t = 300\mu\text{s}$ ),  $OCS_2$  has already completed the switch to  $P_2$  and is ready to transmit. This effectively “hides” the latency of  $OCS_2$  behind the transmission of  $OCS_1$ .
- (3) **Topology Bypassing:** Beyond overlapping, SWOT identifies opportunities to *skip* unnecessary intermediate configurations. In the naive approach, every OCS must strictly follow the sequence  $P_1 \rightarrow P_2 \rightarrow P_3 \dots$ . However, SWOT recognizes that  $OCS_1$  does not need to handle Step 2 ( $P_2$ ) if  $OCS_2$  can absorb that demand. Consequently,  $OCS_1$  transitions directly from  $P_1 \rightarrow P_3$ , completely bypassing  $P_2$ . Similarly,  $OCS_2$  handles Steps 2 and 5 (both  $P_2$ ) while skipping  $P_3$ . This optimization reduces the total number of reconfiguration operations per OCS, directly saving time overhead.

Through this “relay-style” execution—where planes not only overlap tasks but also intelligently skip unnecessary reconfiguration—SWOT reduces the CCT to  $1200\mu\text{s}$ , achieving a **20% speedup** without adding physical resources. The following sections describe how we generalize this intuition into a formal scheduling framework.

### 3.2 SWOT Scheduler: Formulation & Constraints

While the intuition in §3.1 demonstrates the potential of SWOT, applying it to complex algorithms and large clusters requires solving a high-dimensional combinatorial problem. The scheduler must co-optimize traffic distribution and topology transitions while strictly adhering to the physical and logical constraints of the optical cluster.

**3.2.1 Scheduling Properties.** To ensure a valid and executable schedule, our formulation must satisfy three fundamental properties:

- (P1) *Transmission-Reconfiguration Precedence*: Data transmission on a specific OCS plane can only commence after the necessary optical circuit is fully established.
- (P2) *Serial Resource Usage*: A single OCS device cannot perform multiple activities (e.g., transmitting and reconfiguring) simultaneously.
- (P3) *Logical Step Barrier*: To preserve the semantics of collective algorithms, step  $i$  cannot logically begin until step  $i - 1$  is fully resolved across all participating planes.

**3.2.2 MILP Formulation.** We formulate this problem as a Mixed Integer Linear Programming (MILP) model. The complete notation is provided in Table 1.

**Decision Variables.** We introduce two sets of variables that serve as the “control knobs” for our design mechanisms:

- **Message Split** ( $d_{i,j}$ ): The data volume assigned to OCS  $j$  at step  $i$ . This variable enables **Workload Distortion** by allowing  $d_{i,j}$  to deviate from the uniform split ( $m_i/k$ ).
- **Reconfiguration Flag** ( $r_{i,j}$ ): A binary variable indicating if OCS  $j$  reconfigures before step  $i$ . This variable enables **Configuration Bypassing** ( $r_{i,j} = 0$ ) to skip unnecessary latency.

**Optimization Model.** The objective is to minimize the Communication Completion Time (CCT):  
 $\min \text{CCT} = \max_i t_{\text{step}_e_i}$ . The constraints are formulated to enforce properties (P1)-(P3) while enabling asynchronous execution:

$$\left\{ \begin{array}{l} \sum_{j=1}^k d_{i,j} \times u_{i,j} = m_i \quad \forall i \quad (1) \\ t_{\text{end}_{i,j}} - t_{\text{start}_{i,j}} = \frac{d_{i,j}}{B} + T_{\text{lat}} \cdot u_{i,j} \quad \forall i, j \quad (2) \\ t_{\text{recfg}_e_{i,j}} - t_{\text{recfg}_s_{i,j}} = r_{i,j} \cdot T_{\text{recfg}} \quad \forall i, j \quad (3) \\ r_{i,j} \geq u_{i,j} - s_{i,j} \quad \forall i, j \quad (4) \\ |\text{cfg}_i - \text{last\_cfg}_{i,j}| \leq M \cdot (1 - s_{i,j}) \quad \forall i, j \quad (5) \\ t_{\text{prev}_e_{i,j}} = 0 \quad (6) \\ t_{\text{prev}_e_{i,j}} \geq \begin{cases} t_{\text{prev}_e_{i-1,j}} \\ t_{\text{end}_{i-1,j}} \cdot u_{i-1,j} \\ t_{\text{recfg}_e_{i-1,j}} \cdot r_{i-1,j} \end{cases} \quad (7) \\ t_{\text{recfg}_s_{i,j}} \geq t_{\text{prev}_e_{i,j}} \quad (8) \\ t_{\text{start}_{i,j}} \geq t_{\text{recfg}_e_{i,j}} \quad \forall i, j \quad (9) \\ t_{\text{step}_e_i} \geq t_{\text{end}_{i,j}} \cdot u_{i,j} \quad \forall i, j \quad (10) \\ t_{\text{start}_{i,j}} \geq t_{\text{step}_e_{i-1}} \quad \forall i > 1, j \quad (11) \end{array} \right.$$

**3.2.3 Constraint Analysis.** We analyze how these constraints enforce rigorous correctness while unlocking the proposed optimizations:

**1. Flexible Assignment via Traffic Conservation (Eq. 1).** Eq. (1) ensures that the total message  $m_i$  is distributed among active OCSs. Unlike static schemes that enforce equality, this constraint gives the solver the freedom to adjust  $d_{i,j}$  arbitrarily. This mathematical flexibility is the foundation of **Workload Distortion**, allowing the scheduler to sacrifice the transmission time of one plane to buy reconfiguration time for another.

**2. Decoupled Timelines via Serial Resource Usage (Eq. 3–9).** These constraints manage the internal timeline of each OCS  $j$  to satisfy properties  $(P1)$  and  $(P2)$ :

- **Enabling Bypassing:** Eq. (4) and (5) govern the reconfiguration logic. They allow  $r_{i,j} = 0$  (and thus zero latency penalty in Eq. 3) if the current physical configuration matches the requirement ( $s_{i,j} = 1$ ), effectively mathematically realizing **Configuration Bypassing**.
- **Enabling Asynchronous Overlap:** Eq. (7) and (8) define the earliest start time for a new operation based *only* on the previous activity of the *same* OCS. Crucially, Eq. (8) permits  $OCS_j$  to start reconfiguring immediately after its previous task finishes ( $t_{prev\_e,i,j}$ ), regardless of the state of other OCS planes. This local dependency (as opposed to global synchronization) is what formally enables **Asynchronous Overlap**.
- **Ensuring Integrity:** Eq. (9) enforces  $(P1)$ , guaranteeing that transmission ( $t_{start}$ ) never occurs before the circuit is ready ( $t_{reconf\_e}$ ).

**3. Global Synchronization (Eq. 10–11).** While operations within a step are asynchronous, Eq. (10) and (11) enforce  $(P3)$ . They ensure that the logical algorithm structure is preserved by forcing step  $i$  to wait for the completion of step  $i - 1$  across all planes. This represents the boundary condition for our optimization: we maximize overlap *inside* the steps to minimize the waiting time at these barriers.

**3.2.4 Solving Feasibility.** While MILP is computationally intensive, it does not constitute a bottleneck for SWOT in production DML environments. This is supported by three key factors:

- (1) **Offline Amortization:** DML workloads are characterized by highly deterministic and repetitive communication patterns [13]. Consequently, SWOT functions as a one-time *offline* planner. The cost of schedule generation is incurred only during initialization and is amortized over millions of iterations in a training job (often spanning weeks).
- (2) **Relaxed Optimality:** Our objective is not to find the theoretically global optimum, but to find a schedule that significantly outperforms the static and naive baselines. MILP solvers typically find high-quality feasible solutions early in the search process, spending the majority of time closing the “optimality gap”. For SWOT, a “good enough” solution that overlaps 80% of the reconfiguration latency is functionally as valuable as a perfect solution overlapping 100%, provided it meets the time constraints.
- (3) **Empirical Efficiency:** In our extensive evaluation (see §4), we utilized an off-the-shelf open-source solver (CBC via Pulp[21]) with a strict time limit of 120 seconds. Empirical results demonstrate that the solver consistently converges to solutions yielding significant performance gains within this short window, even for large-scale clusters (*e.g.*,  $p = 1024$ ). This confirms that standard solvers are sufficiently efficient for practical deployment without requiring specialized heuristic algorithms.

### 3.3 SWOT Framework & Execution Model

Designed to bridge the gap between static communication libraries and dynamic optical hardware, SWOT operates in two distinct phases: offline planning and runtime coordination.

**Phase 1: Offline Scheduling.** As shown in the top half of Figure 6, the workflow begins with the SWOT Offline Scheduler. Given the predictable nature of DML workloads, the scheduler extracts communication patterns (message sizes, peer ranks) from the model framework and parallelization strategy. It then executes the MILP solver (detailed in §3.2) to generate a synchronized Execution Plan. This plan is a dual-track schedule containing: (1) A *Reconfiguration Sequence* for the Optical Network Controller, specifying when to switch topologies. (2) A *Transmission Sequence* for the computing nodes, specifying data chunks and dependencies.

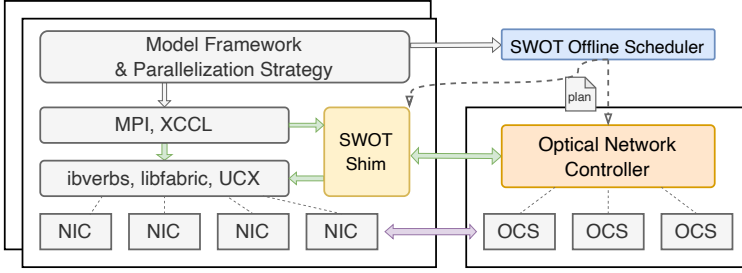


Fig. 6. **System Integration of SWOT.** The framework consists of an Offline Scheduler for plan generation and a runtime Shim layer. The Shim mediates optical hardware with existing communication libraries, ensuring synchronization between data streams (via NICs) and topology reconfiguration (via OCSs).

**Phase 2: Runtime Orchestration via Shim.** At runtime, SWOT introduces a lightweight Shim Layer to orchestrate execution. Rather than modifying the complex internals of lower-level drivers (e.g., `ibverbs`, `UCX`), the Shim is designed as a logical mediation layer that sits alongside standard communication libraries (e.g., `MPI`, `XCCL`).

**Coordination Logic.** The Shim intercepts high-level collective calls and decomposes them into the sequence of Point-to-Point (P2P) micro-operations defined in the Execution Plan. Its primary role is to enforce the *Transmission-Reconfiguration Precedence* (Property P1). Before issuing a data transfer command to the NIC, the Shim verifies the readiness of the corresponding optical path—either via time-based synchronization or explicit signaling from the Optical Network Controller.

**Compatibility.** A key advantage of this design is its compatibility with existing ecosystems. Since the computed schedule ultimately consists of P2P transfers mapped to specific optical planes, the Shim can be realized using standard primitives (e.g., `ncc1Send/ncc1Recv` or `MPI_Isend`). This allows SWOT to leverage the mature, high-performance data paths of existing libraries while transparently injecting the benefits of optical reconfiguration.

## 4 Evaluation

We comprehensively evaluate SWOT to demonstrate its efficiency and scalability across different CC algorithms, with direct comparisons for each primitive. We also investigate its performance under varying network settings, examining the impact of optical resources and reconfiguration speeds on the scheduling strategy.

### 4.1 Experimental Setup

We evaluate SWOT through rigorous numerical simulations. Similar to [33], the communication time is calculated using the  $\alpha - \beta$  model, which accounts for both the fixed latency ( $\alpha$ ) and bandwidth-dependent transmission time ( $\beta$ ). This approach ensures that our evaluation captures realistic transmission behaviors, including serialization overheads and propagation delays, rather than relying solely on ideal bandwidth models.

**Network Topology.** We simulate a representative optical topology (Fig. 2) consisting of  $p$  computing nodes interconnected by  $k$  OCSs. Each node is equipped with  $k$  interfaces, each connected to a distinct OCS. Following common commercial designs [30], we set the OCS reconfiguration delay  $T_{\text{refg}}$  to 200  $\mu\text{s}$ . The impact of reconfiguration latency is further evaluated in § 4.3.2.

**Network Parameters.** To reflect modern hardware capability, we set the total aggregate bandwidth per computing node at 800 Gbps. Consequently, the per-link bandwidth  $B$  is determined by the degree of parallelism, calculated as  $B = 800/k$  Gbps.  $k$  stands for the optical degree, which leverages the breakout capabilities inherent in modern high-performance NICs. To account for

realistic physical layer overheads, we set the end-to-end base latency  $T_{\text{lat}}$  to  $20\mu\text{s}$ , which captures the typical propagation delay and hardware serialization time in data center optical interconnects.

**Solver Configuration.** For the optimization component of SWOT, we employ the Pulp optimizer to solve the MILP formulation. To ensure practical feasibility and fair comparison across all experiments, all schedules are generated with a strict solver time limit of 120 seconds, unless explicitly stated otherwise. This constraint emulates the requirement for rapid schedule generation in production environments.

**Algorithm Selection.** For the algorithm-level evaluation (§ 4.2.1 and § 4.2.2), we select four representative CC algorithms: (1) Rabenseifner’s ReduceScatter; (2) Rabenseifner’s AllReduce; (3) Pairwise All-to-All; and (4) Bruck’s All-to-All [7]. For the primitive-level evaluation (§ 4.2.3), we adopt a “best-of-breed” strategy: we automatically select the collective algorithm that minimizes the estimated CCT for each scheme, ensuring a fair comparison against the best-case static configurations.

**Baseline Methods.** SWOT is compared against three scheduling paradigms: (1) **One-shot:** Full optical circuit pre-configuration with fixed topology; (2) **Strawman-ICR:** Naive intra-collective reconfiguration without overlap optimization [5]; (3) **Ideal:** Communication without any network constraints, operating at maximum aggregated NIC bandwidth.

## 4.2 Performance Analysis

In this section, we conduct a multi-faceted evaluation to quantify the benefits of SWOT. We structure our analysis across three key dimensions:

- (1) **Algorithmic Efficiency:** We examine how SWOT accelerates specific representative algorithms across varying message sizes, highlighting its ability to reduce CCT through overlap scheduling.
- (2) **Cluster Scalability:** We assess the system’s behavior as the cluster size scales, demonstrating SWOT’s advantage in handling increasingly complex traffic patterns.
- (3) **Primitive Performance Envelope:** We evaluate SWOT at the primitive level (*e.g.*, AllReduce, All-to-All). By selecting the best-performing algorithm for each schedule method and network configuration, we demonstrate how SWOT expands the overall performance envelope for fundamental primitives, independent of the underlying algorithmic implementation.

*4.2.1 Collective Operation Efficiency.* Fig. 7 compares SWOT against existing solutions across different CC algorithms. Compared to one-shot, SWOT reduces CCT by up to 84.0%, 83.7%, 72.7%, and 89.7% for Rabenseifner’s ReduceScatter, AllReduce, Pairwise All-to-All, and Bruck’s All-to-All, respectively; similarly, SWOT outperforms Strawman-ICR by up to 89.1%, 87.1%, 89.1%, and 85.4%, respectively. These results demonstrate SWOT’s superiority in accelerating diverse CC algorithms over optical networks. Note that there is a gap between SWOT and the ideal scenario because SWOT must reserve time for optical reconfiguration, and the link bandwidth is not 100% utilized.

Specifically, the experimental results reveal three key observations. (1) **SWOT and Strawman-ICR achieve sublinear scaling**, whereas one-shot shows linear CCT growth as message size increases. This occurs because one-shot’s static pre-allocation activates only the subset of OCSes matching the traffic pattern, wasting the bandwidth of idle links. In contrast, dynamic reconfiguration enables higher network utilization across the communication steps. (2) **Reconfiguration overhead is non-negligible for small messages.** For small messages ( $< 1$  MB in Fig. 7(d)), both Strawman-ICR and SWOT exhibit comparable or higher CCT than one-shot. Reconfiguration overhead rivals transmission duration here, where naive intra-collective reconfiguration scheduling incurs penalties from frequent reconfigurations. *SWOT alleviates this via overlapped reconfiguration-communication technique.* (3) **The performance gap between Strawman-ICR**

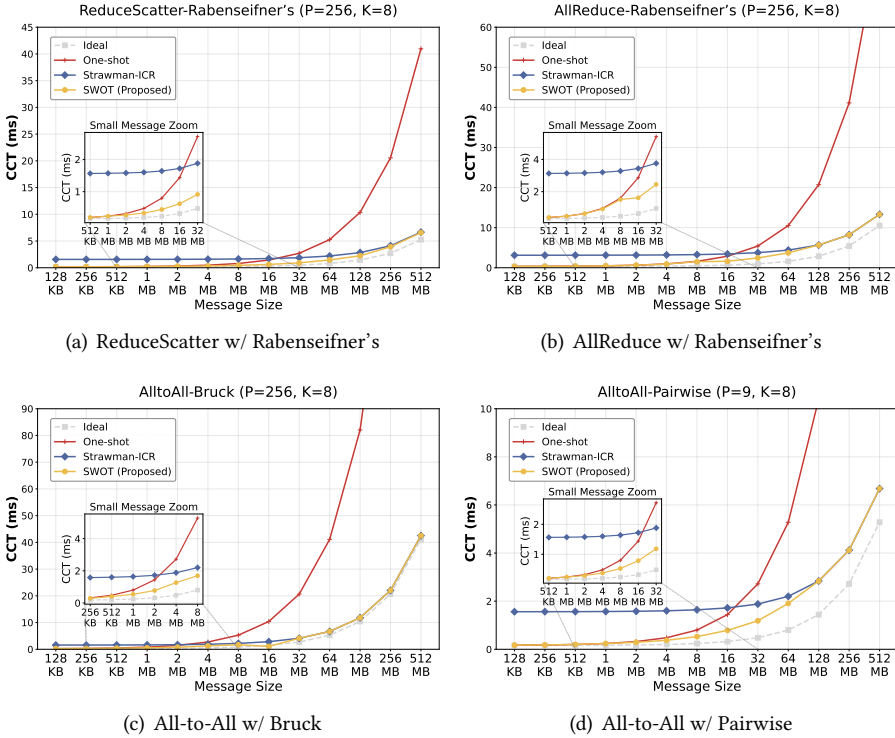


Fig. 7. CCT vs message size for different collective operations algorithm on a dedicated cluster of 256 nodes physically fully connected to 8 OCSs ( $B = 100$  Gbps). 9-node setup for Pairwise due to one-shot scalability constraints. The small plot in the bottom left reports runtime for small message results.

and SWOT narrows with large messages ( $> 64$ MB in Fig 7(d)), as data transmission time becomes the dominant factor.

Furthermore, we observe that **SWOT yields varying improvements depending on the collective algorithm**. Bruck’s All-to-All (Fig. 7(c)) shows relatively lower gains despite higher total data volume due to its limited number of communication phases, which restricts reconfiguration opportunities. In contrast, Pairwise All-to-All (Fig. 7(d)) and Rabenseifner’s AllReduce (Fig. 7(b)) exhibit distinct levels of improvement. Although they share identical data volumes, their distinct configuration sequences and message distributions account for the variation in benefits.

**4.2.2 Cluster Scalability.** Fig. 8 shows CCT scaling with cluster size for Rabenseifner’s AllReduce and Pairwise’s All-to-All operations using 4 OCSs. Key observations include: (1) One-shot supports only up to 16-node clusters for AllReduce and 5-node clusters for All-to-All, as larger deployments exceed its 4-OCS capacity. Both Strawman-ICR and SWOT overcome this by enabling runtime reconfiguration. (2) Larger clusters induce more diverse traffic patterns, increasing reconfiguration overhead in Strawman-ICR. SWOT reduces this overhead by co-optimizing data transfer and optical reconfiguration, improving scalability. Consequently, SWOT’s performance advantage over Strawman-ICR improves with cluster size: for Rabenseifner’s AllReduce, CCT reduction grows from 39.6% at 64 nodes to 46.9% at 512 nodes; for Pairwise All-to-All, improvement rises from 26.0% at 5 nodes to 45.5% at 10 nodes. **Large-scale clusters thus derive greater benefits from SWOT, highlighting its scalability for complex CC algorithms.**

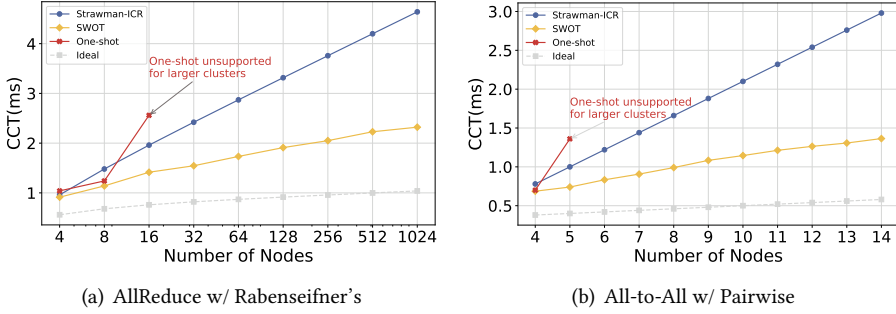


Fig. 8. Impact of cluster size on CCT for different CC algorithm on a dedicated cluster physically fully connected to 4 OCSs ( $B = 200$  Gbps, message size = 32 MB).

4.2.3 *End-to-End Primitive Performance.* SWOT is designed to be algorithm-agnostic: it does not prescribe a specific CC algorithm but rather optimizes the execution of any given algorithm on optical substrates. To validate this, we evaluate the end-to-end performance of two common primitives: AllReduce and All-to-All.

Here we adopt a “best-of-breed” strategy: for each primitive and each data point, we select the specific CC algorithm that yields the lowest CCT for the baseline. We then apply SWOT to this optimal algorithm to measure the performance gain.

This approach ensures that we are comparing against the theoretical performance ceiling of each scheduling paradigm. The results are shown in Figure 9, where the labels above the data points denote the selected best algorithm (e.g., **B** for Bruck, **P** for Pairwise, **RD** for Recursive Doubling, **HD** for Rabenseifner’s, and **DP** for Double Binary Tree). Notably, Double Binary Tree’s performance is highly sensitive to pipeline chunk size. We therefore implemented a heuristic chunk selection strategy derived from the NVIDIA NCCL source code to dynamically tune chunk size based on message volume and cluster scale ( $p$ ).

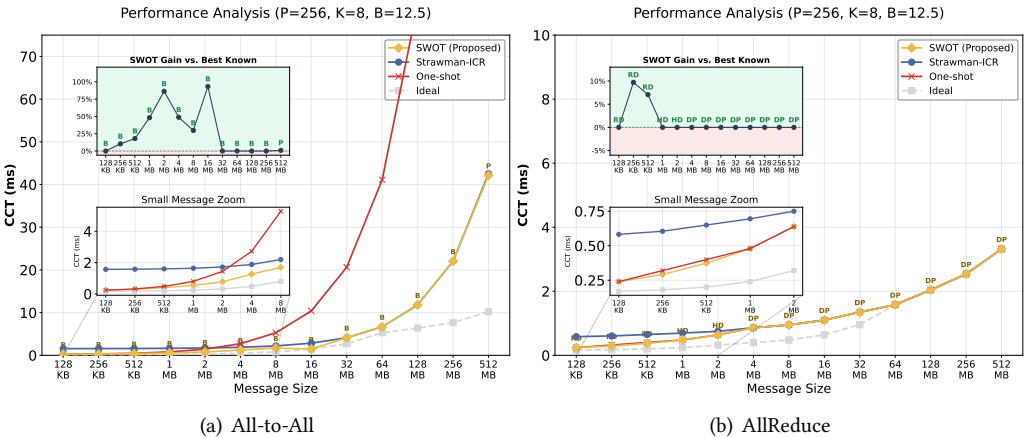


Fig. 9. Normalized CCT for different collective primitives. For each primitive, the results are derived using the best-performing algorithm for the specific configuration. The small plot in the bottom left reports runtime for small messages; top left shows the CCT gain of SWOT compared to the combination of best-known algorithms and scheduling strategies. Letters on top of each datapoint denote the abbreviation of the best-known algorithm.

**All-to-All (Fig. 9(a)): Dominating Dynamic Patterns.** For the All-to-All primitive, which exhibits dense and dynamic traffic patterns, SWOT demonstrates substantial performance gains. As

shown in the top-left zoom-in plot, SWOT achieves a peak speedup of over 93.19% compared to the best-known baseline at medium message sizes (e.g., 16 MB). In this range, the *Bruck* algorithm (**B**) is optimal but requires  $\log N$  reconfiguration steps. SWOT effectively pipelines these reconfigurations, whereas Strawman-ICR incurs heavy switching penalties and one-shot suffers from severe bandwidth fragmentation. At extremely large message sizes (e.g., 512 MB), the *Pairwise* algorithm (**P**) becomes dominant. Here, the transmission time significantly exceeds the reconfiguration latency, causing the gap between schemes to narrow as the system becomes bandwidth-bound.

**AllReduce (Fig. 9(b)): Near-Optimal Static Baselines.** For AllReduce, we observe more modest benefits. The traffic patterns of AllReduce (e.g., Ring, Tree) are inherently sparse and map efficiently to static topologies, allowing the one-shot approach to perform near-optimally. Specifically, SWOT achieves a peak improvement of 7.06%–9.71% in the small-to-medium message regime (256 KB–512 KB) by optimizing the step-wise execution of *Halving-Doubling* (**HD**). For larger messages (> 1 MB), the one-shot approach remains highly competitive, as the DP algorithm can fully saturate the bandwidth of a static topology without requiring runtime reconfiguration.

**Insight: The Potential of Co-Design.** The results above reveal a fundamental limitation: the collective algorithms used in this study (e.g., Bruck, Double Binary Tree) were originally designed under the assumption of a static network. While SWOT extracts performance gains by scheduling these legacy algorithms dynamically, we posit that this is only the tip of the iceberg. A holistic *co-design* of collective algorithms and reconfigurable topology scheduling—where the communication pattern is inherently designed to exploit temporal reconfiguration—would likely yield significantly larger performance gains. This represents a promising and direction for future research.

### 4.3 Impact of System Parameters

In this section, we delve into how physical network parameters dictate the performance gains of SWOT. We investigate the influence of optical degree ( $k$ ) and reconfiguration latency ( $T_{\text{recfg}}$ ) to understand the underlying mechanisms of reconfiguration-communication overlapping.

**4.3.1 Impact of Optical Degree ( $k$ ).** We investigate the impact of the optical degree  $k$  (the number of OCS interfaces per node) on SWOT’s performance. We fix the total bandwidth per node at 800 Gbps and scale  $k \in \{2, 4, 8\}$ , resulting in per-link bandwidths of 400, 200, and 100 Gbps, respectively. The experiments are conducted on a 256-node cluster with a strict solver time limit of 120 seconds. Figure 10 illustrates the improvement over Strawman-ICR. We observe three key trends:

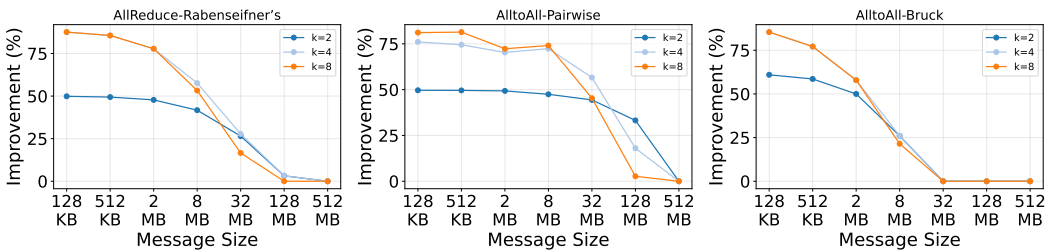


Fig. 10. Impact of optical degree  $k$  on Performance Improvement across different algorithms ( $p = 256$ , Solver Limit = 120s). While higher  $k$  generally improves performance via finer granularity, the exploded search space at  $k = 8$  can lead to sub-optimal solutions under strict time constraints.

**(1) Finer Scheduling Granularity Yields Higher Potential Gains.** In general, increasing  $k$  provides finer scheduling granularity. With more parallel optical lanes, SWOT possesses greater flexibility to pipeline reconfiguration and transmission, effectively minimizing the reconfiguration overhead ratio. **(2) Diminishing Marginal Returns.** Increasing  $k$  exhibits diminishing returns. As shown in Fig. 10, the performance improvement from  $k = 4$  to  $k = 8$  is often marginal. This suggests

a moderate optical degree (e.g.,  $k = 4$ ) suffices to exploit most reconfiguration-communication overlap opportunities; further increases yield limited benefit. **(3) Trade-off between Search Space and Solution Quality.** Contrarily, we observe instances where a higher  $k$  leads to performance degradation. Notably, for the Pairwise and Halving-Doubling algorithms at larger message sizes (e.g., 8 MB), the performance of  $k = 8$  drops below that of  $k = 4$ , and sometimes even below  $k = 2$ . This anomaly is attributed to the exponential growth of the solution space. Under the strict 120-second time limit, the solver may fail to converge to a near-optimal solution for these complex, high-dimensional instances, resulting in sub-optimal schedules.

**4.3.2 Impact of Reconfiguration Latency ( $T_{\text{reconf}}$ ).** We evaluate the robustness of SWOT by varying the reconfiguration latency  $T_{\text{reconf}}$  across four orders of magnitude:  $\{0.02, 0.2, 2.0, 20.0\}$  ms. This range encompasses diverse optical switching technologies, from ultra-fast switches to slower MEMS-based devices. Experiments are conducted on a 256-node cluster with  $k = 4$ . Figure 11 presents the reconfiguration overhead ratio across different message sizes. We highlight two observations:

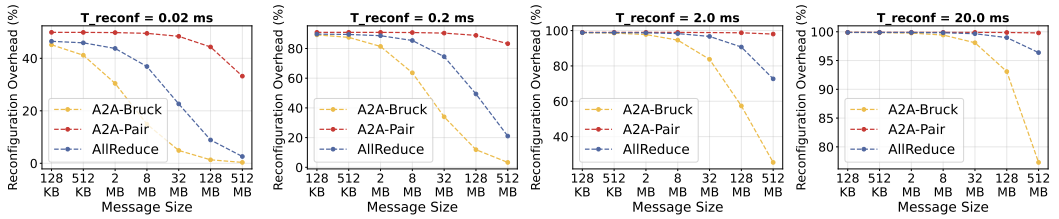


Fig. 11. Reconfiguration Overhead vs. Message Size under varying Reconfiguration Latencies ( $T_{\text{reconf}}$ ). The "knee" of the curve, representing the onset of effective overlapping, shifts to the right as  $T_{\text{reconf}}$  increases, confirming that gains are maximized when transmission time exceeds reconfiguration latency.

**(1) Hardware Robustness across Latency Scales.** SWOT demonstrates significant adaptability across varying  $T_{\text{reconf}}$ . While absolute overhead naturally increases with slower switches (e.g.,  $T_{\text{reconf}} = 20$  ms), the framework consistently identifies valid schedules that maintain correctness. This underscores SWOT's hardware agnosticism, proving its viability not only on cutting-edge experimental hardware but also on cost-effective, higher-latency commercial optical switches.

**(2) The Mechanics of Overlapping: The Critical Ratio.** The results reveal that the efficacy of the overlap technique is fundamentally governed by the ratio between the per-step transmission duration ( $t_{\text{trans}} = m_{\text{step}}/B$ ) and the reconfiguration latency ( $T_{\text{reconf}}$ ). We observe a "critical inflection point" in the overhead curves:

- **Latency-Dominated Regime** ( $t_{\text{trans}} < T_{\text{reconf}}$ ): When message size is small, transmission time is insufficient to cover the reconfiguration delay of the subsequent step. In this regime (the flat plateaus on the left of Fig. 11), the system gain from overlapping is minimal, as the bottleneck is strictly the switching speed.
- **Bandwidth-Dominated Regime** ( $t_{\text{trans}} \geq T_{\text{reconf}}$ ): As message size increases,  $t_{\text{trans}}$  exceeds  $T_{\text{reconf}}$ . The scheduler effectively overlaps OCS reconfiguration latency with ongoing transmissions on other OCSs. As a result, the reconfiguration overhead ratio is greatly reduced.

As  $T_{\text{reconf}}$  increases from 0.2 ms to 20 ms, the inflection point shifts to the right, requiring larger message sizes to achieve effective overlap. Moreover, the improvement rate is algorithm-dependent. Algorithms with larger per-step data chunks (e.g., A2A-Bruck) enter the bandwidth-dominated regime earlier, whereas those with more fragmented traffic patterns (e.g., A2A-Pairwise) require substantially larger messages to generate sufficient transmission time to mask the latency.

This result highlights a key advantage of SWOT: it relaxes the stringent requirement for ultra-low latency optical switches. By effectively hiding latency, SWOT enables high-performance collective communication even on commodity OCS hardware with millisecond-level switching times.

## 5 Related Work

**Optical Interconnects for ML.** Optical switching has been widely explored to accelerate DML. Systems like SiP-ML [16], TopoOpt [28], InfiniteHBD, and Google TPUv4 [14, 34] leverage OCS to build demand-aware topologies. However, they predominantly adopt a “one-shot” strategy, fixing the topology for entire training iterations to avoid reconfiguration overhead. Recent works like ACTINA [29] and MixNet [18] introduce dynamism by reconfiguring between computation phases, yet they still treat collective operations as atomic, static blocks. Crucially, while Athapathu et al. [5] theoretically analyzed intra-collective reconfiguration, they concluded that performance gains are restricted to ultra-fast switches ( $< 500$  ns). SWOT challenges this conclusion, demonstrating that by overlapping reconfiguration with transmission, significant gains are achievable even with commodity microsecond-scale switches.

**Collective Algorithm Synthesis.** Significant research focuses on the design and synthesis of efficient CC algorithms for specific topologies. SCCL [8] pioneered a systematic approach to synthesizing collective algorithms. Subsequent works explored diverse optimization strategies: TACCL [25] improves scalability via communication sketches but trades off schedule quality; TE-CCL [31] adopts a traffic-engineering-based formulation; SyCCL [9] exploits collective symmetries for efficient and accurate schedule synthesis. Notably, Zhao et al. [33] jointly optimize static direct-connect topologies and their corresponding collective schedules at scale.

## 6 Discussions

**Generalization to Multi-dimensional Topologies.** Our current evaluation focuses on a 1D flattened topology where all nodes connect to  $k$  parallel OCS planes. However, production systems like Google’s TPUv4/v5 [14, 34] employ multi-dimensional direct-connect topologies (e.g., 3D Torus) to scale beyond the port-count limits of a single OCS. In such architectures, OCS devices are partitioned by dimensions, providing connectivity only within specific subsets of nodes. Theoretically, SWOT’s framework is compatible with these architectures. However, extending the MILP scheduler to multi-dimensional constraints requires modeling dimension-specific bandwidth limits and routing policies, representing a challenging yet valuable direction for future research.

**Adaptability to non-deterministic and non-uniform collective workloads** While our current work targets predictable and uniform collectives, advanced models like Mixture-of-Experts (MoE) and Deep Learning Recommendation Models (DLRM) present two extra challenges: non-uniformity and unpredictability. However, the core principle of SWOT (intra-collective reconfiguration) remains applicable to non-uniform traffic—it already optimizes for uneven splits. The bottleneck lies in prediction accuracy. Integrating SWOT with runtime traffic predictors (e.g., MixNet [18]) represents a promising direction for handling dynamic sparsity.

**Algorithmic Co-design Opportunities.** SWOT currently acts as an accelerator for existing CC algorithms designed for static networks. While we achieve significant gains by scheduling these legacy algorithms dynamically, this is likely only the tip of the iceberg. A holistic co-design approach, where the collective algorithm itself is synthesized with explicit awareness of SWOT’s overlapping capabilities, could yield even higher performance.

## 7 Conclusion

In this paper, we present SWOT, an intra-collective reconfigurable optical framework that dynamically aligns network resources with the communication demands of individual CC algorithms.

SWOT dedicatedly splits messages, selects target optical topologies, and schedules optical reconfigurations asynchronously to overlap reconfiguration with data transmission. By hiding optical reconfiguration costs, SWOT reduces topology switching overhead while remaining compatible with existing collective libraries. Our evaluation demonstrates up to 89.7% communication time reduction across diverse primitives, with robust performance against varying optical degrees and reconfiguration latencies spanning four orders of magnitude. This work introduces a co-adaptive paradigm between optical networks and dynamic DML communication, offering a potential pathway toward scalable infrastructure for future AI training systems.

**Ethics.** This work does not raise ethical concerns.

## References

- [1] 2025. Broadcom Ethernet Network Adapter User Guide. <https://techdocs.broadcom.com/us/en/storage-and-ethernet-connectivity/ethernet-nic-controllers/bcm957xxx/adapters.html>
- [2] 2025. *Ethernet Adapters and Controllers - FastLinQ Performance NICs - 45000 FastLinQ CNA - Marvell*. <https://www.marvell.com/products/ethernet-adapters-and-controllers/fastlinq-cna-adapters/45000-fastlinq-cna/documents.html>
- [3] Intel 2025. *Intel® Ethernet 800 Series Product Guide*. Intel. <https://www.intel.com/content/www/us/en/content-details/709766/intel-ethernet-800-series-product-guide.html>
- [4] 2025. *Port Splitting Configurations - NVIDIA Docs*. <https://docs.nvidia.com/networking/display/connectx8supernic/port-splitting-configurations>
- [5] Rukshani Athapathu and George Porter. 2025. Reconfigurability within Collective Communication Algorithms. In *Proceedings of the 2nd Workshop on Networks for AI Computing (NAIC '25)*. Association for Computing Machinery, New York, NY, USA, 43–49.
- [6] Hitesh Ballani, Paolo Costa, Raphael Behrendt, Daniel Cletheroe, Istvan Haller, Krzysztof Jozwik, Fotini Karinou, Sophie Lange, Kai Shi, Benn Thomsen, and Hugh Williams. 2020. Sirius: A Flat Datacenter Network with Nanosecond Optical Switching. In *Proceedings of the Annual Conference of the ACM Special Interest Group on Data Communication on the Applications, Technologies, Architectures, and Protocols for Computer Communication (SIGCOMM '20)*. Association for Computing Machinery, New York, NY, USA, 782–797.
- [7] J. Bruck, Ching-Tien Ho, S. Kipnis, E. Upfal, and D. Weathersby. 1997. Efficient Algorithms for All-to-All Communications in Multiport Message-Passing Systems. *IEEE Transactions on Parallel and Distributed Systems* 8, 11 (1997), 1143–1156.
- [8] Zixian Cai, Zhengyang Liu, Saeed Maleki, Madanlal Musuvathi, Todd Mytkowicz, Jacob Nelson, and Olli Saarikivi. 2021. Synthesizing Optimal Collective Algorithms. In *Proceedings of the 26th ACM SIGPLAN Symposium on Principles and Practice of Parallel Programming (PPoPP '21)*. Association for Computing Machinery, New York, NY, USA, 62–75.
- [9] Jiamin Cao, Shangfeng Shi, Jiaqi Gao, Weisen Liu, Yifan Yang, Yichi Xu, Zhilong Zheng, Yu Guan, Kun Qian, Ying Liu, Mingwei Xu, Tianshu Wang, Ning Wang, Jianbo Dong, Binzhang Fu, Dennis Cai, and Ennan Zhai. 2025. SyCCL: Exploiting Symmetry for Efficient Collective Communication Scheduling. In *Proceedings of the ACM SIGCOMM 2025 Conference (SIGCOMM '25)*. Association for Computing Machinery, New York, NY, USA, 645–662.
- [10] Marco Cococcioni and Lorenzo Fiaschi. 2021. The Big-M Method with the Numerical Infinite M. *Optimization Letters* 15, 7 (2021), 2455–2468.
- [11] Manya Ghobadi. 2022. Emerging Optical Interconnects for AI Systems. In *Optical Fiber Communication Conference (OFC) 2022 (Optical Fiber Communication Conference (OFC) 2022)*. Optica Publishing Group, Th1G.1.
- [12] Roger W Hockney. 1994. The Communication Challenge for MPP: Intel Paragon and Meiko CS-2. 20, 3 (1994), 389–398.
- [13] Ziheng Jiang, Haibin Lin, Yinmin Zhong, Qi Huang, Yangrui Chen, Zhi Zhang, Yanghua Peng, Xiang Li, Cong Xie, Shibiao Nong, Yulu Jia, Sun He, Hongmin Chen, Zhihao Bai, Qi Hou, Shipeng Yan, Ding Zhou, Yiyao Sheng, Zhuo Jiang, Haohan Xu, Haoran Wei, Zhang Zhang, Pengfei Nie, Leqi Zou, Sida Zhao, Liang Xiang, Zherui Liu, Zhe Li, Xiaoying Jia, Jianxi Ye, Xin Jin, and Xin Liu. 2024. {MegaScale}: Scaling Large Language Model Training to More than 10,000 {GPUs}. In *21st USENIX Symposium on Networked Systems Design and Implementation (NSDI 24)*. 745–760.
- [14] Norm Jouppi, George Kurian, Sheng Li, Peter Ma, Rahul Nagarajan, Lifeng Nai, Nishant Patil, Suvinay Subramanian, Andy Swing, Brian Towles, Clifford Young, Xiang Zhou, Zongwei Zhou, and David A Patterson. 2023. TPU v4: An Optically Reconfigurable Supercomputer for Machine Learning with Hardware Support for Embeddings. In *Proceedings of the 50th Annual International Symposium on Computer Architecture (ISCA '23)*. Association for Computing Machinery, New York, NY, USA, 1–14.
- [15] Jared Kaplan, Sam McCandlish, Tom Henighan, Tom B. Brown, Benjamin Chess, Rewon Child, Scott Gray, Alec Radford, Jeffrey Wu, and Dario Amodei. 2020. Scaling Laws for Neural Language Models.
- [16] Mehrdad Khani, Manya Ghobadi, Mohammad Alizadeh, Ziyi Zhu, Madeleine Glick, Keren Bergman, Amin Vahdat, Benjamin Klenk, and Eiman Ebrahimi. 2021. SiP-ML: High-Bandwidth Optical Network Interconnects for Machine Learning Training. In *Proceedings of the 2021 ACM SIGCOMM 2021 Conference (SIGCOMM '21)*. Association for Computing Machinery, New York, NY, USA, 657–675.
- [17] Leon, Omid Mashayekhi, Joon Ong, Arjun Singh, Mukarram Tariq, Rui Wang, Jianan Zhang, Virginia Beaugard, Patrick Conner, Steve Gribble, Rishi Kapoor, Stephen Kratzer, Nanfang Li, Hong Liu, Karthik Nagaraj, Jason Ornstein, Samir Sawhney, Ryohei Urata, Lorenzo Vicisano, Kevin Yasumura, Shidong Zhang, Junlan Zhou, and Amin Vahdat. 2022. Jupiter Evolving: Transforming Google's Datacenter Network via Optical Circuit Switches and Software-Defined Networking. In *Proceedings of the ACM SIGCOMM 2022 Conference (SIGCOMM '22)*. Association for Computing Machinery, New York, NY, USA, 66–85.
- [18] Xudong Liao, Yijun Sun, Han Tian, Xinchen Wan, Yilun Jin, Zilong Wang, Zhenghang Ren, Xinyang Huang, Wenxue Li, Kin Fai Tse, Zhizhen Zhong, Guyue Liu, Ying Zhang, Xiaofeng Ye, Yiming Zhang, and Kai Chen. 2025. MixNet: A Runtime Reconfigurable Optical-Electrical Fabric for Distributed Mixture-of-Experts Training. In *Proceedings of*

- the ACM SIGCOMM 2025 Conference (SIGCOMM '25)*. Association for Computing Machinery, New York, NY, USA, 554–574.
- [19] Hong Liu, Ryohei Urata, Kevin Yasumura, Xiang Zhou, Roy Bannon, Jill Berger, Pedram Dashti, Norm Jouppi, Cedric Lam, Sheng Li, Erji Mao, Daniel Nelson, George Papen, Mukarram Tariq, and Amin Vahdat. 2023. Lightwave Fabrics: At-Scale Optical Circuit Switching for Datacenter and Machine Learning Systems. In *Proceedings of the ACM SIGCOMM 2023 Conference (ACM SIGCOMM '23)*. Association for Computing Machinery, New York, NY, USA, 499–515.
  - [20] William M. Mellette, Rob McGuinness, Arjun Roy, Alex Forencich, George Papen, Alex C. Snoeren, and George Porter. 2017. RotorNet: A Scalable, Low-complexity, Optical Datacenter Network. In *Proceedings of the Conference of the ACM Special Interest Group on Data Communication (SIGCOMM '17)*. Association for Computing Machinery, New York, NY, USA, 267–280.
  - [21] Stuart Mitchell, Michael OSullivan, and Iain Dunning. 2011. Pulp: A Linear Programming Toolkit for Python. 65 (2011). <https://www.dit.uoi.gr/e-class/modules/document/file.php/216/PAPERS/2011.%20PuLP%20-%20A%20Linear%20Programming%20Toolkit%20for%20Python.pdf>
  - [22] Rolf Rabenseifner. 2004. Optimization of Collective Reduction Operations. In *Computational Science - ICCS 2004*, Takeo Kanade, Josef Kittler, Jon M. Kleinberg, Friedemann Mattern, John C. Mitchell, Moni Naor, Oscar Nierstrasz, C. Pandu Rangan, Bernhard Steffen, Madhu Sudan, Demetri Terzopoulos, Dough Tygar, Moshe Y. Vardi, Gerhard Weikum, Marian Bubak, Geert Dick Van Albada, Peter M. A. Sloot, and Jack Dongarra (Eds.). Vol. 3036. Springer Berlin Heidelberg, Berlin, Heidelberg, 1–9.
  - [23] Peter Sanders, Jochen Speck, and Jesper Larsson Träff. 2025. Two-Tree Algorithms for Full Bandwidth Broadcast, Reduction and Scan. 35, 12 (2025), 581–594. <https://doi.org/10.1016/j.parco.2009.09.001>
  - [24] Daniele De Sensi, Tommaso Bonato, David Saam, and Torsten Hoefler. 2024. Swing: Short-cutting Rings for Higher Bandwidth Allreduce. In *21st USENIX Symposium on Networked Systems Design and Implementation (NSDI 24)*. 1445–1462.
  - [25] Aashaka Shah, Vijay Chidambaram, Meghan Cowan, Saeed Maleki, Madan Musuvathi, Todd Mytkowicz, Jacob Nelson, Olli Saarikivi, and Rachee Singh. 2023. {TACCL}: Guiding Collective Algorithm Synthesis Using Communication Sketches. In *20th USENIX Symposium on Networked Systems Design and Implementation (NSDI 23)*. 593–612.
  - [26] Guanhua Wang, Shivaram Venkataraman, Amar Phanishayee, Jorgen Thelin, Nikhil Devanur, and Ion Stoica. 2020. Blink: Fast and Generic Collectives for Distributed ML. In *Conference on Machine Learning and Systems (MLSys 2020)*.
  - [27] Hao Wang, Han Tian, Jingrong Chen, Xinchun Wan, Jiacheng Xia, Gaoxiong Zeng, Wei Bai, Junchen Jiang, Yong Wang, and Kai Chen. 2024. Towards {Domain-Specific} Network Transport for Distributed {DNN} Training. In *21st USENIX Symposium on Networked Systems Design and Implementation (NSDI 24)*. 1421–1443.
  - [28] Weiyang Wang, Moein Khazraee, Zhizhen Zhong, Manya Ghobadi, Zhihao Jia, Dheevatsa Mudigere, Ying Zhang, and Anthony Kewitsch. 2023. {TopoOpt}: Co-optimizing Network Topology and Parallelization Strategy for Distributed Training Jobs. In *20th USENIX Symposium on Networked Systems Design and Implementation (NSDI 23) (NSDI'23)*. 739–767.
  - [29] Zhenguang Wu, Benjamin Klenk, Larry Dennison, and Keren Bergman. 2025. ACTINA: Adapting Circuit-Switching Techniques for AI Networking Architectures. In *Proceedings of the International Conference for High Performance Computing, Networking, Storage and Analysis (New York, NY, USA, 2025-11-15) (SC '25)*. Association for Computing Machinery, 1211–1222. <https://dl.acm.org/doi/10.1145/3712285.3759842>
  - [30] Xuwei Xue, Shaojuan Zhang, Bingli Guo, Wei Ji, Rui Yin, Bin Chen, and Shanguo Huang. 2023. Optical Switching Data Center Networks: Understanding Techniques and Challenges. arXiv:2302.05298 [cs, eess]
  - [31] Xuting Liu, Behnaz Arzani, Siva Kesava Reddy Kakarla, Liangyu Zhao, Vincent Liu, Miguel Castro, Srikanth Kandula, and Luke Marshall. 2024. Rethinking Machine Learning Collective Communication as a Multi-Commodity Flow Problem. In *Proceedings of the ACM SIGCOMM 2024 Conference (ACM SIGCOMM '24)*. Association for Computing Machinery, New York, NY, USA, 16–37.
  - [32] Zhisheng Ye, Wei Gao, Qinghao Hu, Peng Sun, Xiaolin Wang, Yingwei Luo, Tianwei Zhang, and Yonggang Wen. 2024. Deep Learning Workload Scheduling in GPU Datacenters: A Survey. *Comput. Surveys* 56, 6 (2024), 146:1–146:38.
  - [33] Liangyu Zhao, Siddharth Pal, Tapan Chugh, Weiyang Wang, Jason Fantl, Prithwish Basu, Joud Khoury, and Arvind Krishnamurthy. 2025. Efficient {Direct-Connect} Topologies for Collective Communications. In *22nd USENIX Symposium on Networked Systems Design and Implementation (NSDI 25)*. 705–737.
  - [34] Yazhou Zu, Alireza Ghaffarkhah, Hoang-Vu Dang, Brian Towles, Steven Hand, Safeen Huda, Adekunle Bello, Alexander Kolbasov, Arash Rezaei, Dayou Du, Steve Lacy, Hang Wang, Aaron Wisner, Chris Lewis, and Henri Bahini. 2024. Resiliency at Scale: Managing {Google's} {TPUV4} Machine Learning Supercomputer. In *21st USENIX Symposium on Networked Systems Design and Implementation (NSDI 24)*. 761–774.